ELSEVIER

Desalination 207 (2007) 144–152

DESALINATION

www.elsevier.com/locate/desal

Hydraulic permeability of polydispersed cake layers: an analytic approach

Albert S. Kim*, Aileen N.L. Ng

Civil and Environmental Engineering, University of Hawaii at Manoa, 2540 Dole Street, Honolulu, HI 96822, USA
Tel. +1 (808) 956-3718; Fax: +1 (808) 956-5014; email: AlbertSK@hawaii.edu

Received 8 December 2005; Accepted 5 April 2006

Abstract

An analytic method is introduced to calculate hydraulic permeability of porous media composed of polydispersed spheres with log-normal and normal (Gaussian) distributions of particle sizes. From the comparison of the permeability for the two particle-size distributions, it was observed that a medium with normally distributed particle sizes consistently has a lower permeability than a medium with log-normally distributed particle sizes. This phenomenon is due to the larger number of smaller particles in the normal distribution, which results in greater cake resistance. The specific resistance of the cake layer is computed by taking the inverse of the permeability.

Keywords: Poly-dispersed cake layer; Cake resistance; Hydraulic permeability; Particle-size distribution; Log-normal distribution; Normal (Gaussian) distribution

1. Introduction

One of the major problems encountered in applications of membrane filtration technology is permeate flux decline due to deleterious fouling phenomena [1,2]. In microfiltration (MF) and ultrafiltration (UF) processes, particle deposition results in cake formation on membrane surfaces and hence generates additional hydraulic resistance to water permeation. While a plethora of fouling studies have proposed basic mechanisms of the fouling phenomena and have attempted to explain the permeate flux decline behavior, both experimental and theoretical approaches are somewhat limited to ideal and well-controlled cases. An assumption commonly made, which rarely reflects real situations, is that particles suspended in feed water are monodispersed [3–14].

Several models have been introduced to compute the specific resistance (i.e., inverse hydraulic permeability) of porous media composed of

*Corresponding author.

equal-sized spherical particles [15–21]. The Carman-Kozeny model [15] is based on the definition of hydraulic diameter and the empirical condition of touching spheres. Happel's cell model [17] maps a sphere-packed porous medium to a single solid sphere located in a concentric spherical cell on which tangential stress is nullified. Although both models can be used to generate good estimates of the hydraulic resistance of cake layers, they are fully based on cake layers composed of mono-dispersed spherical particles.

In reality, feed water contains a diversity of particles that vary in composition and size. Poly-dispersity of particle sizes plays an important role in the hydraulic resistance of cake layers. A few quality studies have been conducted to examine the effects of particle poly-dispersity on water permeation in MF and UF processes [22,23]. Fundamental expressions of the poly-dispersed cake permeability are, however, still lacking in the literature. In this light, the current study derives expressions for the permeability of media composed of poly-dispersed spherical particles by considering two typical ideal particle-size distributions: the log-normal and normal (Gaussian) distributions.

2. Theory

When a single spherical particle is located in a uniform flow field, the hydrodynamic drag force exerted on the particle can be rigorously represented by Stokes' law [24,25]:

$$F_{\text{Stokes}} = 6\pi\mu a U \tag{1}$$

where μ is the absolute fluid viscosity, a is the particle radius, and U is the uniform fluid velocity. If N particles of different sizes form a cake layer on the membrane surface, the total drag force exerted on the cake layer can be represented as

$$F = \sum_{i=1}^{N} 6\pi\mu a_i \Omega_i U \tag{2}$$

where i(=1,2,...,N) is the particle index, and Ω_i (>1) is a hydraulic factor that corrects the drag force experienced by particle i in the cake layer [15–21]. From Eq. (2), it is evident that the hydro-dynamic force on a sphere in the presence of adjacent particles is higher than that experienced by an isolated spherical particle. The hydro-dynamic force density is attained by dividing Eq. (2) by the total volume V of the cake layer, which includes void spaces in addition to the volume occupied by the spheres. Equating the force density to the pressure gradient across the cake layer gives [26,27]:

$$\frac{F}{V} = \frac{\sum_{i=1}^{N} 6\pi\mu a_i \Omega_i U}{V} = \frac{\mu U}{\kappa} \tag{3}$$

where κ is the cake permeability (i.e., inverse specific cake resistance). Due to the incompressibility of the fluid, U is interpreted to be the approaching velocity at the top of the cake layer and hence the permeate velocity. The total cake volume can be expressed as

$$V = \frac{\sum_{i=1}^{N} \frac{4\pi}{3} a_i^3}{\phi} \tag{4}$$

where ϕ is the overall volume fraction of the cake layer. Substituting Eq. (4) into Eq. (3) and solving for the permeability yields

$$\kappa = \frac{2\left(\frac{1}{N}\sum_{i=1}^{N} a_i^3\right)}{9\phi\left(\frac{1}{N}\sum_{i=1}^{N} a_i \Omega_i\right)} = \frac{2\langle a^3\rangle}{9\phi\langle a\Omega\rangle} \tag{5}$$

If the assumption is made that the hydrodynamic forces acting on all the particles in the cake layer are uniformly corrected by the hydraulic factor, i.e.,

$$\langle a\Omega\rangle \simeq \langle a\rangle\langle\Omega\rangle \simeq \langle a\rangle\Omega(\phi) \tag{6}$$

then Eq. (5) can be rewritten as

$$\kappa = \frac{2a_{\text{eff}}^2}{9\phi\Omega} \tag{7}$$

where

$$a_{\text{eff}} = \sqrt{\frac{\langle a^3\rangle}{\langle a\rangle}} \tag{8}$$

which is termed the effective radius. Thus, a sphere-packed medium of different particle sizes is hydraulically equivalent to a medium composed of mono-dispersed particles with the effective particle radius a_{eff}. The specific cake resistance is computed by simply taking the inverse of the permeability:

$$r_c = \frac{1}{\kappa} \tag{9}$$

Furthermore, the cake layer resistance R_c can be found by multiplying the specific resistance by the thickness of the cake layer.

In the present study, the log-normal and normal (Gaussian) distributions are employed as model distributions, and the effective radius and hydraulic permeability for both distributions are calculated and compared (see following sections).

2.1. Log-normal distribution

The log-normal distribution of particle radii is given by

$$L(a)\mathrm{d}a = \frac{1}{\sqrt{2\pi}\beta a}\exp\left(-\frac{\left[\ln(a/a_0)\right]^2}{2\beta^2}\right)\mathrm{d}a \tag{10}$$

where $L(a)\mathrm{d}a$ is the fraction of particles with radii between a and $a+\mathrm{d}a$, and a_0 and β are parameters that can be determined experimentally. By the mathematical definition of

$$\langle a^n\rangle \equiv \int_{a=0}^{\infty} a^n L(a)\mathrm{d}a \tag{11}$$

one can obtain

$$\langle a^n\rangle = a_0^n \exp\left(\frac{n^2\beta^2}{2}\right) \tag{12}$$

and

$$\langle a\rangle = a_0\, e^{1/2\beta^2} \tag{13}$$

$$\langle a^2\rangle = a_0^2 e^{2\beta^2} = \langle a\rangle^2 e^{\beta^2} \tag{14}$$

$$\langle a^3\rangle = a_0^3 e^{9\beta^2/2} = \langle a\rangle^3 e^{3\beta^2} \tag{15}$$

Using Eqs. (13) and (15), the effective radius can be expressed as

$$a_{\text{eff}} = \sqrt{\frac{\langle a^3\rangle}{\langle a\rangle}} = \langle a\rangle e^{\frac{3}{2}\beta^2} \tag{16}$$

Therefore, the permeability of the cake layer composed of log-normally distributed particle sizes is

$$\kappa_L = \frac{2}{9}\frac{\langle a\rangle^2}{\phi\Omega}e^{3\beta^2} \tag{17}$$

and the specific cake resistance is

$$r_{c,L} = \frac{1}{\kappa_L} \tag{18}$$

Using Eqs. (13) and (14), the standard deviation of the particle radii is expressed as

$$\begin{aligned}\sigma = \sqrt{\langle a^2 \rangle - \langle a \rangle^2} &= a_0 \sqrt{e^{\beta^2}\left(e^{\beta^2} - 1\right)} \\ &= \langle a \rangle \sqrt{\left(e^{\beta^2} - 1\right)}\end{aligned} \tag{19}$$

With experimentally determined values for the mean $\langle a \rangle$ and standard deviation σ of the log-normally distributed particle radii, Eqs. (13) and (19) can be used to calculate the values of a_0 and β. The cake permeability can then be calculated with Eq. (17), knowing the values of β and ϕ.

2.2. Normal distribution

The normal (Gaussian) distribution of particle radii is given by

$$N(a)\mathrm{d}a = \frac{1}{\sqrt{2\pi}\sigma} \exp\left(-\frac{\left(a - \langle a \rangle\right)^2}{2\sigma^2}\right)\mathrm{d}a \tag{20}$$

where $N(a)\mathrm{d}a$ is the fraction of particles with their radii between a and $a+\mathrm{d}a$, and $\langle a \rangle$ and σ are the mean and standard deviation, respectively, of the normal particle-size distribution. Again, the mathematical definition of Eq. (11) is used here:

$$\langle a^n \rangle = \int_0^\infty a^n N(a)\mathrm{d}a \tag{21}$$

and the following approximation is made:

$$\langle a^n \rangle \approx \int_{-\infty}^\infty a^n N(a)\mathrm{d}a \tag{22}$$

Eq. (22) is valid when $\langle a \rangle$ is greater than 2σ since the range of the normal distribution is roughly 4σ [28]. Solving Eq. (22) for $n = 3$ yields

$$\langle a^3 \rangle = \langle a \rangle \left(\langle a \rangle^2 + 3\sigma^2\right) \tag{23}$$

The effective radius of normally distributed particle-sizes is then

$$a_{\mathrm{eff}} = \sqrt{\langle a \rangle^2 + 3\sigma^2} \tag{24}$$

Therefore, the hydraulic permeability of normally distributed spherical particles is

$$\kappa_N = \frac{2\langle a \rangle^2}{9\phi\Omega}\left(1 + \frac{3}{4}\left(\frac{2\sigma}{\langle a \rangle}\right)^2\right) \tag{25}$$

and the specific cake resistance is

$$r_{c,N} = \frac{1}{\kappa_N} \tag{26}$$

Similar to the log-normal case, the permeability (and the specific cake resistance) can be obtained from the mean and standard deviation of the particle sizes and the average cake volume fraction.

3. Results and discussion

A comparison is made between cake layers of log-normally versus normally distributed particles with regard to permeability using the same mean and standard deviation of particle sizes for the two distributions. The ratio of the permeabilities is derived by substituting Eqs. (13) and (19) into Eq. (25) and dividing Eq. (25) by Eq. (17):

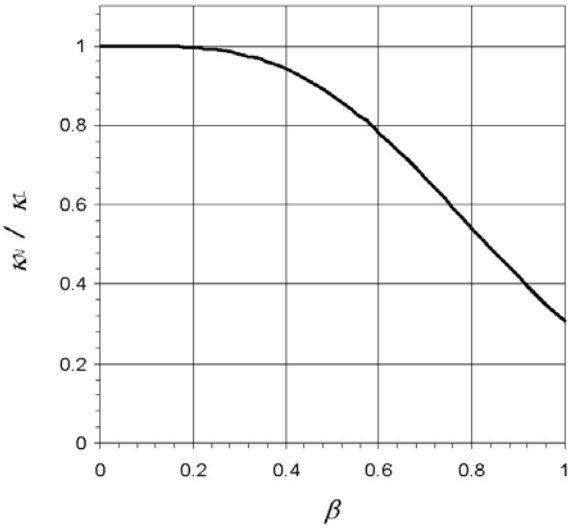

Fig. 1. Ratio of the normal to log-normal permeability as a function of β.

$$\frac{\kappa_N}{\kappa_L} = e^{-3\beta^2}\left(3e^{\beta^2} - 2\right) \tag{27}$$

Fig. 1 shows the ratio in Eq. (27) as a function of β and reveals that the normal distribution always exhibits lower permeability than the log-normal distribution for $\beta > 0$. In other words, a cake layer composed of normally distributed particles will have higher specific resistance in comparison to one composed of log-normally distributed particles with the same mean and standard deviation.

The mean-scaled distributions are defined as

$$\langle a\rangle L(r) = \frac{1}{\sqrt{2\pi}\beta r} \exp\left(-\frac{1}{2\beta^2}\left[\frac{\beta^2}{2} + \ln(r)\right]^2\right) \tag{28}$$

$$\langle a\rangle N(r) = \frac{1}{\sqrt{2\pi\left(e^{\beta^2}-1\right)}} \exp\left(-\frac{(r-1)^2}{2\left(e^{\beta^2}-1\right)}\right) \tag{29}$$

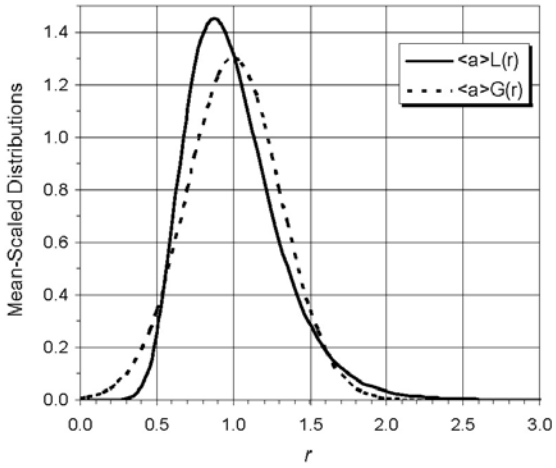

Fig. 2. Mean-scaled log-normal [$\langle a\rangle L(a)$] and normal [$\langle a\rangle N(a)$] distributions as a function of $r(=a/\langle a\rangle)$ with $\beta = 0.3$.

where $r=a/\langle a\rangle$. The two scaled distributions in Eqs. (28) and (29) are plotted in Fig. 2 with $\beta = 0.3$. The log-normal distribution has a higher peak at $r = e^{\frac{-3}{2}\beta^2}$ (≤ 1) for $\beta > 0$, and the normal distribution (of which its peak stays at $r = 1$) has a longer tail near zero radius. This indicates that the normal distribution has a larger number of smaller particles in comparison to the log-normal distribution with the same mean and standard deviation.

For a cake layer composed of equal-sized particles (i.e., with zero standard deviation) that are homogeneously and isotropically distributed with a certain volume fraction, the cake permeability is proportional to the square of the particle radius. Therefore, a cake layer of smaller monodispersed particles has a lower permeability, i.e., higher specific resistance. Note that, in this study, the spatial fraction of volume occupied by each particle is assumed to be identical and is used as the average cake volume fraction. Therefore, the contribution to the specific resistance by the left-tail portion of particle-size distributions (of Fig. 2) is of greater significance. For a cake layer composed of polydispersed particleswith a given back thickness and porosity, smaller

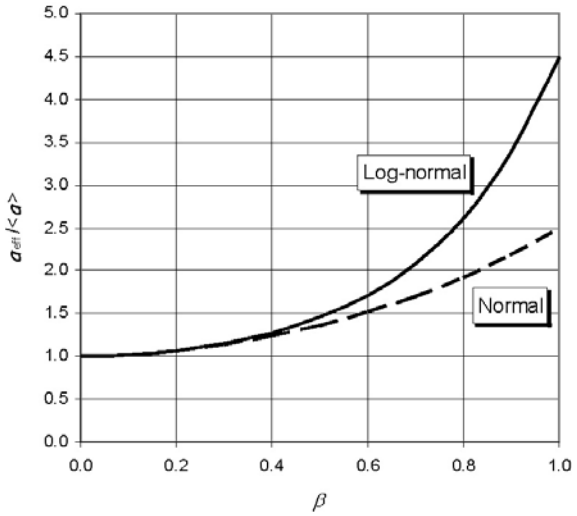

Fig. 3. Dimensionless effective radii $a_{eff}/\langle a\rangle$ of log-normal and normal distributions as a function of β.

particles contribute tremendously to a larger cake resistance. This explains the lower permeability observed for the normal distribution in Fig. 1.

Another way to explain the role of smaller particles is to compare effective radii in Eqs. (16) and (24), for log-normal and normal distributions, respectively, with the same mean and standard deviation of particle sizes. The dimensionless radii, $a_{eff}/\langle a\rangle$, for the two distributions are plotted in Fig. 3 as sole functions of β. Fig. 3 illustrates that, in general, the effective radius a_{eff} of the log-normal distribution is always larger than that of the normal distribution. For example, if $\beta = 0.8$, the effective radius of the log-normal distribution is 1.36 times greater than that of the normal distribution. This implies that while a cake layer composed of normally distributed spherical particles can be mapped into a mono-dispersed cake layer of particle radius a', a log-normally distributed cake layer can be equi-valently treated as a mono-dispersed cake layer composed of particle radius $1.36a'$. Note that the permeability is proportional to the square of the particle radius.

The grand assumption employed in this study, i.e., the equal spatial fraction for each particle, was motivated by Soppe's work [29], which showed that the vertical density profile of sediments (i.e., polydispersed sphere packing) is uniform and homogeneous regardless of its polydispersity, i.e., the standard deviation of particle size in a Gaussian distribution. Estimation of drag forces exerted on a swarm of polydispersed particles is another important task because the cake permeability depends on the sum of the drag forces (see Eq. (3)). Possible methods for estimation include microscale computational approaches to hydrodynamics such as the collocation method [30,31], Stokesian dynamics [32–34], and lattice Boltzmann method [35]. Each method has advantages and disadvantages to acutely evaluate drag forces exerted on a swarm of particles. However, the number of particles used in each method is limited to a few hundred [33,36].

Although rapid calculation algorithms and parallel computational methods are under vigorous development [37], the rigorous estimation of cake permeability in actual practice is still a formidable task. In this light, we believe that the current work provides an unprecedented level of analytic expression for specific cake resistance of polydispersed cake layers.

When polydispersed particles deposit on the membrane surface and form a certain cake layer, the spatially uniform distribution, assumed in this study, may not be fully valid. Indirect experimental studies [29,38,39] show that the size as well as mass density of particles influence the degree and manner of stratification of cake layers. This phenomenon can become much more complex when the feed solution contains several different kinds of particulate materials with their own polydispersity. When shear-induced diffusion [8,40–46] plays an important role in particle back-diffusion from the membrane surface to the bulk phase, the bottom section of the cake layer will consist mainly of small particles. If the cake structure is noticeably stratified, the total resistance can be estimated simply using the resistance-in-series model. In this case, larger

particles would not contribute noticeably to the cake resistance because the major resistance mostly stems from deposited small particles. On the other hand, if entropic (Brownian) influence dominates the hydrodynamic effect, then the cake structure will have a random, well-mixed, (macroscopically) uniform distribution of polydispersed particles throughout the entire layer. Our approach can fit well into the latter case, in which larger particles play a beneficial role in permeate production.

4. Concluding remarks

It was shown that, with regard to permeability, a porous medium packed with polydispersed spheres can be characterized as a medium composed of mono-dispersed particles with an effective particle radius $a_{\text{eff}} = \sqrt{\langle a^3 \rangle / \langle a \rangle}$. Expressions for the permeability were derived for the cases of log-normal and normal (Gaussian) particle-size distributions.

Comparison of the two permeability expressions showed that a medium of particles with normally distributed particle sizes always exhibits a higher cake resistance than a medium consisting of log-normally distributed particles sizes when their mean and standard deviation values are identical. This comparative analysis holds greater validity when the mean of the particle sizes is larger than twice the standard deviation.

Finally, the lower permeability for the normal particle-size distribution is due to the greater number of smaller particles (in the distribution), which dominates the overall cake resistance.

Acknowledgments

This work was supported by a grant from the US National Science Foundation Faculty Early Career (CAREER) Development Program (CTS04-49431) and the US Geological Survey, through the Water Resources Research Center, University of Hawaii at Manoa, Honolulu. This is contributed paper CP-2006-08 of the Water Resource Research Center.

References

[1] M. Mulder, Basic Principles of Membrane Technology, Kluwer Academic, Boston, MA, 1996.
[2] American Water Works Association Research Foundation, Water Treatment Membrane Processes, McGraw-Hill, New York, 1996.
[3] F.W. Altena and G. Belfort, Lateral migration of spherical particles in porous channels: Application to membrane filtration, Chem. Eng. Sci., 39 (1985) 343–355.
[4] C.A. Romero and R.H. Davis, Experimental verification of the shear-induced hydrodynamic diffusion model of crossflow microfiltration, J. Membr. Sci., 62 (1991) 249–273.
[5] L.F. Song and M. Elimelech, Theory of concentration polarization crossflow filtration, J. Chem. Soc. Faraday Trans., 91 (1995) 3389–3398.
[6] S. Hong, R.S. Faibish and M. Elimelech, Kinetics of permeate flux decline in crossflow membrane filtration of colloidal suspensions, J. Coll. Interface Sci., 196 (1997) 267–277.
[7] R.S. Faibish, M. Elimelech and Y. Cohen, Effect of interparticle electrostatic double layer interactions on permeate flux decline in crossflow membrane filtration of colloidal suspensions: An experimental investigation, J. Coll. Interface Sci., 204 (1998) 77–86.
[8] S. Chellman and M.R. Wiesner, Evaluation of crossflow filtration models based on shear-induced diffusion and particle adhesion: Complications induced by feed suspension polydispersity, J. Membr. Sci., 138 (1998) 83–97.
[9] A.S. Kim and E.M.V. Hoek, Cake structure in dead-end membrane filtration: Monte Carlo simulation, Environ. Eng. Sci., 19 (2002) 373–386.
[10] J.C. Chen, M. Elimelech and A.S. Kim, Monte Carlo simulation of colloidal membrane filtration: Model development with application to characterization of colloid phase transition, J. Membr. Sci., 255 (2005) 291–305.
[11] H.Y. Ng and M. Elimelech, Influence of colloidal

fouling on rejection of trace organic contaminants by reverse osmosis, J. Membr. Sci., 244 (2004) 215–226.
[12] J.C. Chen and A.S. Kim, Monte Carlo simulation of colloidal membrane filtration: Principal issues of modeling, Adv. Coll. Interface Sci., 119 (2006) 35–53.
[13] S. Lee, J. Cho and M. Elimelech, Combined influence of natural organic matter (NOM) and colloidal particles on nanofiltration membrane fouling, J. Membr. Sci., 262 (2005) 27–41.
[14] Q. Li and M. Elimelech, Synergistic effects in combined fouling of a loose nanofiltration membrane by colloidal materials and natural organic matter, J. Membr. Sci., 278 (2006) 72–82.
[15] P.C. Carman, Fluid flow through a granular bed, Trans. Inst. Chem. Eng., 15 (1937) 150–156.
[16] H.C. Brinkman, On the permeability of media crossing of closely packed porous particles, Appl. Sci. Res., A1 (1947) 81.
[17] J. Happel, Viscous flow in multiparticle systems: Slow motion of fluids relative to beds of spherical particles, AIChE J., 4 (1958) 197–201.
[18] J. Happel and H. Brenner, Low Reynolds Number Hydrodynamics, Prentice-Hall, Englewood Cliffs, NJ, 1965.
[19] I.D. Howells, Drag due to the motion of a Newtonian fluid through a sparse random array of small fixed rigid objects, J. Fluid Mech., 64 (1974) 449–475.
[20] E.J. Hinch, An averaged-equation approach to particle interactions in a fluid suspension, J. Fluid Mech., 83 (1977) 695–720.
[21] S. Kim and W.B. Russel, Modeling of porous media by renormalization of the Stokes equations, J. Fluid Mech., 154 (1985) 269–286.
[22] S.-Y. Lu and C.-M. Tsai, Membrane microstructure resulting from deposition of polydisperse particles, J. Membr. Sci., 177 (2000) 55–71.
[23] N.N. Kramadhati, M. Mondor and C. Moresoli, Evaluation of the shear-induced diffusion model for the microfiltration of polydisperse feed suspension, Sep. Pur. Tech., 27 (2002) 11–24.
[24] R.B. Bird, W.E. Stewart and E.N. Lightford, Transport Phenomena, Wiley, New York, 1960.
[25] H. Lamb, Hydrodynamics, Dover Publications, New York, 1932.
[26] W.B. Russel, D.A. Saville and W.R. Schowalter, Colloidal Dispersions. Cambridge Univ. Press, New York, 1989.
[27] L. Gmachowski, Flow drag in polydisperse systems, Water Res., 32 (1998) 2655–2659.
[28] W. Mendenhall, R.J. Beaver and B.M. Beaver, Introduction to Probability and Statistics, 11th ed., Brooks/Cole, Pacific Grove, CA, 2003.
[29] W. Soppe, Computer simulation of random packings of hard spheres, Powder Technology, 62 (1990) 189–196.
[30] P. Ganatos, R. Pfeffer and S. Weinbaum, A numerical solution technique for three-dimensional stokes flows, with application to the motion of strongly interacting spheres in a plane, J. Fluid Mech., 84 (1978) 79–111.
[31] Q. Hassonjee, P. Ganatos and R. Pfeffer, A strong-interaction theory for the motion of arbitrary three-dimensional clusters of spherical particles at low Reynolds number, J. Fluid Mech., 197 (1988) 1–37.
[32] J.F. Brady and G. Bossis, Stokesian dynamics, Ann. Rev. Fluid Mech., 20 (1988) 111–157.
[33] A.S. Kim and K.D. Stolzenbach, The permeability of synthetic fractal aggregates with realistic three-dimensional structure, J. Coll. Interface Sci., 253 (2002) 315–328.
[34] P.J. Mitchell and D.M. Heyes, Stokesian dynamics simulations of colloids under shear, Molecular Simulation, 15 (1995) 361.
[35] A. Adrover and M. Giona, Hydrodynamic properties of fractals: Application of the lattice Boltzmann equation to transverse flow past an array of fractal objects, Inter. J. Multiphase Flow, 23 (1997) 25–35.
[36] A.S. Kim and K.D. Stolzenbach, Aggregate formation and collision efficiency in differential settling, J. Coll. Interface Sci., 271 (2004) 110–119.
[37] A. Sierou and J.F. Brady, Accelerated Stokesian dynamics simulations, J. Fluid Mech., 448 (2001) 115–146.
[38] A.P.J. Breu, H.M. Ensner, C.A. Kruelle and I. Rehberg, Reversing the brazil-nut effect: Competition between percolation and condensation, Phys. Rev. Lett., 90 (2003) 014302.
[39] J.B. Knight, H.M. Jaeger and S.R. Nagel, Vibration-induced size separation in granular media: The convection connection, Phys. Rev. Lett., 70 (1993) 3728–3731.
[40] D. Leighton and A. Acrivos, Measurement of the

shear induced coefficient of self-diffusion in concentration suspensions of spheres, J. Fluid Mech., 177 (1987) 109–131.
[41] R.H. Davis and D.T. Leighton, Shear-induced transport of a particle layer along a porous wall, Chem. Eng. Sci., 42 (1987) 275–281.
[42] R.H. Davis and S.A. Birdsell, Hydrodynamic model and experiments for crossflow microfiltration, Chem. Eng. Commun., 49 (1987) 217–234.
[43] C.A. Romero and R.H. Davis, Global model of crossflow microfiltration based on hydrodynamic particle diffusion, J. Membr. Sci., 39 (1988) 157–185.
[44] R.H. Davis and J.D. Sherwood, A similarity solution for steady-state crossflow microfiltration, Chem. Eng. Sci., 45 (1990) 3203–3209.
[45] M. Mondor and C. Moresoli, Experimental verification of the shear-induced hydrodynamic diffusion model of crossflow microfiltration, with consideration of the transmembrane pressure axial variation, J. Membr. Sci., 175 (2000) 119–137.
[46] S. Sethi and M.R. Wiesner, Modeling of transient permeate flux in cross-flow membrane filtration incorporating multiple particle transport mechanisms, J. Membr. Sci., 136 (1997) 191–205.